Gravitational collapse of matter in the presence of quintessence and phantomlike scalar fields

Priyanka Saha[*]
Department of Physics, Indian Institute of Technology, Kanpur, Kanpur 208016, India

Dipanjan Dey[†]
Department of Mathematics and Statistics, Dalhousie University, Halifax, Nova Scotia B3H 3J5, Canada

Kaushik Bhattacharya[‡]
Department of Physics, Indian Institute of Technology, Kanpur, Kanpur 208016, India

(Received 7 June 2023; accepted 7 September 2023; published 11 October 2023)

In this work, we propose a model of the gravitational collapse of dark matter in the presence of quintessence or phantomlike scalar fields. Our treatment is based on the principles of general relativity up to virialization. We have chosen a spherical patch that starts to collapse gravitationally as it happens in top-hat collapse. It is seen that although the dark matter sector collapses the dark energy sector does keep a profile that is almost similar to the dark energy profile for the background expanding Friedmann-Lemaitre-Robertson-Walker (FLRW) universe for suitable model parameters. It is observed that in order to formulate the problem in the general relativistic setting one has to abandon the idea of a closed FLRW isolated collapsing patch. General relativity requires an external generalized Vaidya spacetime to be matched with the internal spherical patch whose dynamics is guided by the FLRW metric. It is shown that almost all collapses are accompanied by some flux of matter and radiation in the generalized Vaidya spacetime. Some of the spherical regions of the Universe are seen not to collapse but expand eternally, producing voidlike structures. Whether a spherical region will collapse or expand depends upon the initial values of the system and other model parameters. As this work shows that collapsing structures must emit some form of radiation, this may be taken as an observational signature of our proposal.

DOI: 10.1103/PhysRevD.108.084025

I. INTRODUCTION

The formation of structure in a homogeneous and isotropic universe is always an interesting and evergreen topic in astrophysics and cosmology. In the standard picture, the seed for structure formation in cosmology comes from linear perturbation theory. During or after recombination the cosmological perturbations, for some modes, start to grow and does not remain strictly linear. These modes act as seeds for future structure formation in the Universe. Some of these perturbation modes move out of the linear paradigm and enter the nonlinear mode where different physical principles are operational. Just before entering the nonlinear regime Jeans instability [1,2] and other effects guide the formation of structures. Gravitationally bound structures, from the cluster of galaxies scales to much lower scales, are supposed to have been born due to nonlinear instabilities. In the standard picture of structure formation, it is assumed that primarily the dark matter sector plays the most important role. The dark matter sector is supposed to be composed of a fluid with zero pressure which follows the gravitational potential produced by a marginally denser region and tries to collapse about those regions. The baryonic matter follows the dark matter flow [3–6]. One of the most important semirelativistic methods used to study structure formation is called the top-hat collapse [7]. In this collapse process, it is assumed that if in some closed region of the cosmos, the density of dark matter has exceeded the background matter density then a collapse follows. In top-hat collapse, the closed overdense region at first expands following the background expansion, but this expansion halts at a certain moment due to gravity and there is a turnaround. Following the turnaround, the closed region starts to collapse. A pure general relativistic top-hat collapse generally produces a singularity as the end state, since the collapsing matter is homogeneous and dustlike [8]. However, in astrophysics, it is assumed that much before the formation of a singularity the collapsing fluid virializes. The virialized end state of the collapse signifies structure formation.

[*]priyankas21@iitk.ac.in
[‡]kaushikb@iitk.ac.in
[†]deydipanjan7@gmail.com

n this sense, the top-hat collapse is a semirelativistic process where people use a semi-Newtonian paradigm to interpret the end phase of the collapse.

Traditionally one does not take into account the role of the cosmological constant, Λ, in the structure formation process. Some authors have tried to incorporate the effects of such a constant in the gravitational collapse process [9–12]. Traditional ΛCDM models have their own difficulties [13,14], and consequently, the dynamical dark energy models based on scalar fields have been introduced. One of the most widely used scalar fields in this paradigm is the quintessence field. Phantomlike scalar fields, with a negative kinetic term, also is used to model dark energy [15–19]. In this paper, we will mainly be working with these two types of scalar fields. Our main goal is to study the gravitational collapse process in a two-component universe, with dark matter and a scalar field acting as source of dynamic dark energy. Many authors have attempted such a problem in various forms [20–24]. In almost all of the attempts the authors never used a formal general relativistic approach although they used one or two equations that can only be found in a general relativistic setting. The main reason for such a purely phenomenological approach by the previous authors is primarily based on the following reason. If one wants to apply general relativistic treatment for the gravitational collapse of a closed spherical region then one has to start with the closed Friedmann-Lemaitre-Robertson-Walker (FLRW) spacetime with some matter inside the closed region. This closed region does not exchange energy with the outside as this spacetime is assumed to be "closed" and acts as an isolated system. If this closed region undergoes a gravitational collapse, as in top-hat collapse, then the energy density of the matter inside grows as the region shrinks as that is the only way the energy of matter can be conserved. On the other hand in a two-component system, where one of the components can be a dark energy candidate, this logic may not apply as the dark energy sector may remain homogeneous and unclustered. By unclustered dark energy, we mean that the energy density of dark energy practically remains the same as that of the expanding background FLRW spacetime. In simple terms, the dark energy sector may not collapse at all following the dark matter partner inside the closed region. In such a case energy conservation becomes problematic and the problem becomes paradoxical. To evade this problem, previous authors have used a pure phenomenological method. In this method, one does not perceive the problem relativistically, where one uses an FLRW metric with a positive spatial curvature constant and then writes down the Friedmann equations. The first Friedmann equation (containing the square of the first derivative of the local scale factor) particularly becomes problematic as it requires an estimate of all the known energy sources inside the spherical patch. As energy may not be conserved, this equation becomes redundant. Mostly all of the previous works in this field only use the other Friedmann equation containing the second derivative of the scale factor and consider it as a second-order ordinary differential equation in time and solve it with appropriate initial conditions.

We have addressed the above-mentioned problem in a more relativistic way. As it is known that for unclustered dark energy, the scalar field sector does not collapse, we expect that this sector primarily leaks out of the boundary of the closed, positively curved spacial region. To incorporate such an idea we match the internal FLRW patch with a generalized Vaidya spacetime before the internal spacetime closes (the internal radial distance marker is less than one). As a result of this we predict the emission of radiation from the boundary of the collapsing region, this radiation is naturally obtained in generalized Vaidya spacetimes. The two spacetimes are matched at a timelike hypersurface using the standard junction conditions of general relativity. The matching of the spacetimes solves the issue of nonconservation of energy in the closed patch as in the modified scenario the spherical patch is radiating energy outside and ideally does not remain an isolated patch anymore. In our model, the collapsing dark matter cloud affects the dark energy density locally as the spherical region under collapse forces the dark energy sector to radiate. This model is natural in the sense that the effect of a gravitational collapse does not go unnoticed in the dark energy sector, it reacts to the collapse by transforming locally into radiation although its energy density follows the energy density of the background spacetime. We think this is the first serious attempt to produce a formal general relativistic paradigm of the spherical collapse of dark matter in the presence of dark energy.

Although we have tried to formally establish a general relativistic attempt to tackle the problem of the spherical collapse of matter in the presence of dark energy we do not fully extend the relativistic formalism up to the formation of the singularity which is inevitable in such situations. The primary reason for using a more phenomenological process, to end the collapse, is related to the fact that large-scale structures exist and perhaps they are produced from some virialization process. The complete understanding of the general relativistic version of the Newtonian virialization process remains elusive. Efforts to comprehend the equilibrium process during gravitational collapse within the framework of general relativity have been limited. In a publication by Dey *et al.* [25], a comprehensive and dynamic solution based on general relativity is presented, illustrating a gravitational collapse that ends in an equilibrium state. However, it is important to note that the authors do not assert in that paper that this equilibrium state serves as the direct general relativistic equivalent of the Newtonian virialization state. In [26], Meyer *et al.* present a general relativistic virial theorem based on the Tolman-Oppenheimer-Volkoff (TOV) solution for homogeneous,

perfect-fluid spheres constructed for the Einstein–de Sitter and ΛCDM cosmologies. However, in that paper, the authors do not show how a gravitationally collapsing matter cloud ultimately settles down to the virialization state. They consider an approximately equilibrated system when the vrialization process starts. The equilibrium condition is obtained using the TOV equation for a spherically symmetric static spacetime which is seeded by dust and Λ-dark-energy-like fluid. The authors in that paper do not describe any solution of a dynamical system that ultimately satisfies the time-independent TOV equation at the virialized state. In another work [27], Friedman and Stergioulas introduce a definition of the virial theorem in the context of stationary spacetimes. This matter is extensively covered in Sec. III.3 of their monograph. An in-depth examination into the derivation of the relativistic virial condition for a dynamic spacetime, building upon the condition introduced in the monograph, would undeniably offer a valuable area for exploration. This investigation may shed light on the behavior of rotating relativistic stars under dynamic conditions and contribute to our understanding of their complex nature. However, in this paper, our prime intention is to show the evolution leading to a final virialized state of such a dynamical system which is composed of dust and a minimally coupled scalar field. Our radiating collapsing structure inevitably must virialize at some point in time and after that time the system does not remain relativistic. Virialization by itself is not built in the collapsing process, one has to bring in this pseudo-Newtonian concept to explain the existence of large-scale gravitationally bound objects. In the cases of collapse in the presence of unclustered dark energy, the dark matter sector primarily collapses and virializes whereas the dark energy sector does not virialize. Although the dark energy sector does not virialize it does affect the virialization process of the dark matter sector. Virialization at the end of the collapse does not deter us from using general relativistic methods to unravel the collapsing process. At this point, we want to specify briefly why general relativity is important in our case. The points are as follows:

(i) Any gravitational collapse of matter is intrinsically relativistic as it ends either in a black hole formation or a naked singularity. The physics near black holes or naked singularities can only be tackled through general relativity. Although for phenomenological reasons our specific collapse ends in a virialized state, one can use our method to tackle the full collapse scenario where virialization does not happen.

(ii) All the treatments of gravitational collapse, till now, utilizes some of the assumptions and equations of general relativity and avoids the full relativistic machinery. These methods appear incomplete fundamentally and our attempt to fully represent the problem in the general relativistic setting gives a proper logical completion of the previous attempts.

In all the cases of spherical collapse, which we have studied in this paper, the dark energy component remains primarily unclustered and homogeneous for some suitable small values of parameters in our model. Our attempt to study collapse in such two-component systems does not only produce unclustered dark energy, in some situations, it is seen that the closed, spherical region does not proceed to a collapse at all. In these cases, we have an eternal expansion of a small local spherical patch in the background of the spatially flat FLRW spacetime. These regions act like voids as the matter density inside them decreases. The dark energy density in these patches exceeds the dark energy density of the background and consequently, we can say that clustered dark energy can also be produced in our model. Whether a spherical patch will end up in a virialized state or an expanding phase depends upon the parameters of the theory and initial conditions. In these expanding regions the dark matter density remains a factor of 10 smaller than the background spacetime for some time. Ultimately as these patches expand the matter density drops. The dark energy density remains less than the background dark energy density for quintessence fields. For phantom fields the dark energy density in the spherical patch tends to be more in the voids.

The work in this paper is organized in the following way. In Sec. II we elaborately discuss the semi-Newtonian theory of virialization in a two-component universe where the two components are related to the dark matter sector and the dark energy sector. We call this treatment semi-Newtonian as we use the language of Newtonian potentials although the energy conservation equations are obtained from an expanding universe paradigm. In Sec. III we present the general relativistic formalism for our work. This section contains the junction conditions used to join a collapsing/expanding closed FLRW spacetime with the generalized Vaidya spacetime. Section IV presents the basic equations which guide the collapse of a spherical FLRW patch in the presence of a quintessence/phantomlike scalar field and dark matter. In Sec. V we have presented the results obtained from the calculations in the previous section. This section shows the details of the various collapsing processes. Section VI gives a summary of the work presented in this paper. Throughout the paper, we use a system of units in which the velocity of light and the universal gravitational constant (multiplied by 8π), are both set equal to unity.

II. VIRIALIZATION STATE OF DARK MATTER IN THE PRESENCE OF DARK ENERGY

The total gravitational potential of the overdense region of a two-fluid system consisting of dark matter (DM) and dark energy (DE) can be written as [28]

$$V_T = \frac{1}{2}\int_v \rho_{\rm DM}\phi_{\rm DM}dv + \frac{1}{2}\int_v \rho_{\rm DM}\phi_{\rm DE}dv + \frac{1}{2}\int_v \rho_{\rm DE}\phi_{\rm DM}dv + \frac{1}{2}\int_v \rho_{\rm DE}\phi_{\rm DE}dv, \quad (1)$$

where $\phi_{\rm DM}$ and $\phi_{\rm DE}$ are the gravitational potentials of dark matter and dark energy, respectively, and $\rho_{\rm DM}$ and $\rho_{\rm DE}$ are the energy density of dark matter and dark energy, respectively. The integration is done over the whole volume (v) of the spherical overdense region. The nonzero values of the four integrations written above can be used to classify the two-fluid system into the following four distinguishable scenarios,

(i) In the first scenario, the dark energy effect is totally neglected considering only the first integration in Eq. (1) is nonzero. In this case, the spherical overdensities of dark matter behave like an isolated subuniverse and virialize at a certain radius [7].
(ii) If only the first two integrations in Eq. (1) contribute to the total gravitational potential of the overdense region, then it can be shown that there exists a non-negligible effect of dark energy which affects the virialization process of the spherically symmetric overdense regions of dark matter. In this scenario, dark energy cannot cluster and virialize with dark matter, and therefore, the dark energy density inside the overdense region is similar to the external dark energy density. Hence, this type of model is known as the homogeneous dark energy model [23,29–31].
(iii) In the third scenario, dark energy does not virialize with dark matter though it can cluster inside the overdense regions. In this scenario, it is considered that from the starting point of the matter-dominated era, dark energy moves synchronously with the dark matter on both the Hubble scale and the galaxy cluster scale. This scenario is known as the clustered dark energy scenario [21,25,28,32–34].
(iv) At last, in the fourth scenario, dark energy can cluster and also virializes with dark matter inside the spherical overdense regions [28].

If we consider no influence of dark energy in the evolution of the dark matter overdensities, then as mentioned previously, the first integration of Eq. (1) contributes to the total gravitational potential of the overdense regions. This scenario is described by the top-hat collapse model, where one self-gravitating fluid, inside a spherical overdense region, virializes [7]. In the top-hat collapse model, the overdense region expands first with the background but at a slower rate than that of the background, and then after a certain turnaround radius ($R_{\rm max}$), the overdense region starts collapsing. At the turnaround radius, momentarily the kinetic energy of the overdense region becomes zero, and the total gravitational potential energy (V_T) of the region becomes the total energy (E_T) of the same at that moment. The total energy inside the spherical overdense region, when it reaches the turnaround radius ($R_{\rm max}$), is

$$E_T|_{t=t_{\rm max}} = V_T = \frac{1}{2}\int_{v_{\rm max}} \rho_{\rm DM}\phi_{\rm DM}dv = -\frac{3M^2}{5R_{\rm max}}, \quad (2)$$

where $t_{\rm max}$ is the turnaround time. Here M is the total mass inside the spherical over dense region. A more detailed intuitive description of this mass will be presented in the next section. At the virialization time $t = t_{\rm vir}$, the total kinetic energy of the overdense region $E_{KE}|_{t_{\rm vir}} = -\frac{V_T|_{t_{\rm vir}}}{2}$. Therefore, at the virialization time, the total energy of the overdense region $E_T|_{t_{\rm vir}} = \frac{V_T|_{t_{\rm vir}}}{2}$. Hence, using energy conservation, one can show that the spherically symmetric overdensities virialize when $\eta = \frac{R_{\rm vir}}{R_{\rm max}} = 0.5$. In order to model the dynamics of the overdense region, if one uses the closed FLRW spacetime, then it can be shown that $t_{\rm vir} = 1.81 t_{\rm max}$.

In [23,29], the authors investigated the cosmological scenario where the dark energy is homogeneous, i.e., the internal and external dark energy densities are the same. In [29], the authors studied the effect of the cosmological constant on the virialization of the spherical overdensities, whereas in [23], the authors consider the homogeneous quintessence dark energy model. As previously mentioned, in the homogeneous dark energy scenarios, the dark energy does not cluster and virialize inside the spherical overdensities of dark matter, however, the virialization process of the overdensities is modified since there exist a nonzero energy density and negative pressure of dark energy, and this effect of dark energy can be realized by the different values of η. For the homogeneous dark energy scenario, the total potential energy of the overdense region can be written as [28]

$$V_T = \int_v \rho_{\rm DM}\phi_{\rm DM}dv + \int_v \rho_{\rm DM}\phi_{\rm DE}dv, \quad (3)$$

which gives

$$V_T = -\frac{3M^2}{5R}\left[1 - \frac{q}{2}(1+3\omega)\left(\frac{\bar{a}}{\bar{a}_{\rm max}}\right)^{-3(1+\omega)}\left(\frac{R}{R_{\rm max}}\right)^3\right], \quad (4)$$

where ω is the equation of state of dark energy, assumed to be a constant, and $q = \left(\frac{\rho_{\rm DE}}{\rho_{\rm DM}}\right)_{t=t_{\rm max}}$, which is the ratio of energy densities of dark energy and dark matter inside the spherical overdense regions at the turnaround time $t = t_{\rm max}$. Here and throughout the paper, a and $\bar{a}$ represent the scale factor of the spherical overdense region and the background, respectively. Since the physical radius $R = ra(t)$, at the turnaround time, when the overdense region reaches its maximum physical radius, the scale

factor of the overdense region also reaches its upper limit $a_{\max}$, and at that moment, the scale factor of background is $\bar{a}_{\max}$. At the virialization time $t = t_{\rm vir}$, the scale factors of the overdense region and background become $a_{\rm vir}$ and $\bar{a}_{\rm vir}$, respectively. Using Eq. (4) and the virialization condition $(V_T + \frac{1}{2}R\frac{\partial V_T}{\partial R})_{t=t_{\rm vir}} = (V_T)_{t=t_{\max}}$, we can get the following cubic equation of η:

$$4Q\eta^3\left(\frac{\bar{a}_{\rm vir}}{\bar{a}_{\max}}\right)^{-3(1+\omega)} - 2\eta(1+Q) + 1 = 0, \tag{5}$$

where $Q = -(1+3\omega)\frac{q}{2}$. It can be verified that for the vanishing value of q (i.e., neglecting the dark energy effect), the solution of the above equation is $\eta = 0.5$, which we obtained earlier for the top-hat collapse model. For a homogeneous cosmological constant model, where $\omega = -1$, the above cubic equation for η becomes [29,30]:

$$4q\eta^3 - 2\eta(1+q) + 1 = 0. \tag{6}$$

If we consider small value of q, then the solution of the above equation for η can be written as [30]

$$\eta = 0.5 - 0.25q - 0.125q^2 + \mathcal{O}(q^3), \tag{7}$$

which implies the value of η is always less than 0.5 for models involving the cosmological constant. The presence of Λ makes the overdense regions collapse more to attain the virialization state.

In the homogeneous dark energy model, since the background universe continues expanding after the virialization of the overdense regions, the density of the dark energy (with $\omega \neq -1$) in the virialized overdense region also changes with time, and this is a big problem with the homogeneous dark energy model. This problem is discussed elaborately in [28]. This problem does not appear for models involving the cosmological constant since the density of dark energy always remains constant in such cases. The aforementioned problem is resolved in clustered dark energy models, where, at the galaxy cluster scale, dark energy can cluster and virialize inside the overdense regions. In this scenario, the total gravitational potential energy of the spherical overdense regions can be written as [28]

$$V_T = -\frac{3M^2}{5R} - (2+3\omega)\frac{3M^2}{5R}q\left(\frac{R}{R_{\max}}\right)^{-3\omega} - (1+3\omega)\frac{3M^2}{5R}q^2\left(\frac{R}{R_{\max}}\right)^{-6\omega}, \tag{8}$$

where each of the integrations in Eq. (1) has nonzero value. Using the virialization condition and the above expression of the total gravitational potential energy one can get the following equation for η [28]

$$[1 + (2+3\omega)q + (1+3\omega)q^2]\eta - \frac{1}{2}(2+3\omega)(1-3\omega)q\eta^{-3\omega} - \frac{1}{2}(1-6\omega)(1+3\omega)q^2\eta^{-6\omega} = \frac{1}{2}. \tag{9}$$

There exists another scenario where the dark energy only can cluster inside the spherical overdensities; however, it cannot virialize at that scale. For this scenario, the total potential energy of the spherical regions can be written as

$$V_T = -\frac{3M^2}{5R}\left[1 + q\left(\frac{R}{R_{\max}}\right)^{-3\omega}\right], \tag{10}$$

from which we get the following equation for η [28]:

$$\eta(1+q) - \frac{q}{2}(1-3\omega)\eta^{-3\omega} = \frac{1}{2}. \tag{11}$$

Figure 1(a) depicts how much the value of η deviates from 0.5 for different values of q if we do not neglect the dark energy effect in the evolution of the spherical overdense regions. In that figure, the brown line shows how η changes with q in those scenarios where dark energy can cluster and virialize inside the overdense regions of dark matter. For this scenario, one can verify that η is always greater than 0.5. However, in the case where clustered dark energy cannot virialize, the virialized radius of the spherical overdense region becomes smaller than half of the turnaround radius (i.e., $\eta < 0.5$) which is shown by the blue line in Fig. 1(a). For both these cases, the equation of the state of dark energy is $\omega = -0.75$, and that is relevant for the quintessencelike scalar field. On the other hand, the green curve in Fig. 1(a) shows $\eta < 0.5$ for the case involving the cosmological constant, however, the value of η in this scenario is less than that in the scenario where dark energy can cluster but cannot virialize. In Fig. 1(b), we show a similar thing for $\omega = -1.5$ which is allowed for phantomlike scalar field. It is evident from the figure that the behavior of η in this scenario, with $\omega = -1.5$, differs from the previous scenario with $\omega = -0.75$. Specifically, when the phantomlike scalar field is capable of clustering and virializing, the value of η is greater compared to the quintessencelike scalar field scenario where clustering and virialization occur. In contrast, when considering the scenario where clustered dark energy cannot virialize, the value of η for the phantomlike scalar field is smaller compared to both the quintessencelike scalar field scenario and the scenario arising due to the cosmological constant case. Therefore, we can see that the presence of negative pressure in the dark energy fluid can create distinguishable large-scale structures of dark matter.

In the next section, we use a two-fluid model to describe one of the cosmological scenarios discussed above, where

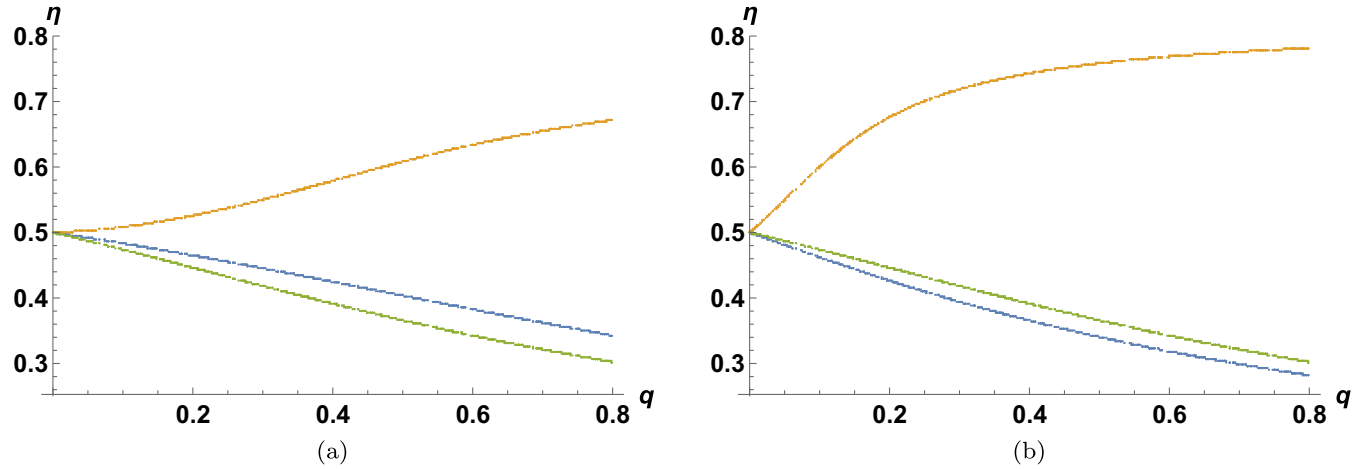

FIG. 1. Figures illustrate the variation of η with q, where $\eta = \frac{R_{\rm vir}}{R_{\rm max}}$ and $q = \left(\frac{\rho_{\rm DE}}{\rho_{\rm DM}}\right)_{t=t_{\rm max}}$, for the following three scenarios: (a) Dark energy is capable of clustering and virializing with dark matter, represented by the brown curve. (b) Dark energy can cluster but cannot virialize within the overdense region, depicted by the blue curve. (c) In the case of a cosmological constant, shown by the green curve. In the first figure (from left), we consider $\omega = -0.75$, which is relevant for quintessencelike scalar field. For the second figure, we consider $\omega = -1.5$, which is relevant for a phantomlike scalar field.

the dark energy is homogeneous and it influences the collapsing dynamics of the overdense dark matter region.

III. GRAVITATIONAL COLLAPSE IN THE PRESENCE OF DUSTLIKE MATTER AND A SCALAR FIELD

As we discussed in the previous section, in this paper, we study the dynamics of a perfect fluid made of dustlike matter and a scalar field [$\phi(t)$] in order to understand the structure formation of dark matter in the presence of dark energy. Since we consider a minimally coupled scalar field with the dustlike matter, the energy-momentum tensor of the resultant fluid ($T^{\mu\nu}$) can be written as the sum of the energy-momentum tensors of the scalar field and the matter:

$$T^{\mu\nu} = (T^{\mu\nu})_m + (T^{\mu\nu})_\phi, \tag{12}$$

where $(T^{\mu\nu})_m$ and $(T^{\mu\nu})_\phi$ correspond to the energy-momentum tensor of dustlike matter and the scalar field, respectively. Therefore, $(T^\mu_\nu)_\phi = \mathrm{diag}(-\rho_\phi, \mathrm{p}_\phi, \mathrm{p}_\phi, \mathrm{p}_\phi)$ and $(T^\mu_\nu)_m = \mathrm{diag}(-\rho_m, 0, 0, 0)$. Here, we consider the collapsing fluid is homogeneous and spherically symmetric. In order to model the dynamics of the overdense region of dark matter in the presence of dark energy, we use closed FLRW spacetime:

$$ds^2 = -dt^2 + \frac{a^2(t)}{1-kr^2}dr^2 + r^2a^2(t)(d\theta^2 + \sin^2\theta d\Phi^2), \tag{13}$$

where $a(t)$ is the scale factor of the overdense region and the constant k can be $0, \pm 1$. If $k = 0$, then we have a flat spatial part whereas negative and positive k imply an open or closed spatial section. We could have taken the metric of the overdense region as a spatially flat FLRW metric, in that case, there will be no turnaround radius. We want to generalize the top-hat collapse in the presence of dark energy and for this, we require a turnaround. For a continual gravitational collapse, singularity forms when the scale factor $a(t)$ becomes zero at a comoving time t_s. At the initial stage of the gravitational collapse ($t = 0$), $a(t)$ can attain any positive definite value that can always be rescaled to one. Therefore, we consider $a(t = 0) = 1$. Since dark matter and dark energy should also be present in the background of the overdense regions, we model the background by the above-mentioned two-fluid model, and we describe the dynamics of the background using flat FLRW spacetime:

$$ds^2 = -dt^2 + \bar{a}^2(t)dr^2 + r^2\bar{a}^2(t)(d\theta^2 + \sin^2\theta d\Phi^2), \tag{14}$$

where, as mentioned before, the scale factor of the background is denoted by $\bar{a}(t)$.

In the present paper, as stated above, we describe the dynamics of the overdense region by closed FLRW spacetime, and the background is modeled by flat FLRW spacetime. However, in order to describe a matter flux through the boundary of the overdense region, in the immediate neighborhood of the overdense region, we consider an external generalized Vaidya spacetime [35]. It should be noted that we do not consider Vaidya spacetime as a background spacetime. The background at the Hubble scale is modeled by flat FLRW spacetime. Vaidya spacetime is used only to describe the local dynamics of matter around the boundary of the overdense patches.

The boundary of the overdense region is a timelike hypersurface $\Sigma = r - r_b = 0$, and the dynamical spacetime structure that we consider here is internally ($\mathcal{V}^-$) closed FLRW metric and externally ($\mathcal{V}^+$) exploding generalized Vaidya spacetime:

$$dS_-^2 = -dt^2 + a^2(t)\left(\frac{dr^2}{1-r^2} + r^2 d\Omega^2\right), \\ = -dt^2 + a^2(t)d\Psi^2 + a^2(t)\sin^2\Psi d\Omega^2, \quad (15)$$

$$dS_+^2 = -\left(1 - \frac{2M(r_v, v)}{r_v}\right)dv^2 - 2dvdr_v + r_v^2 d\Omega^2, \quad (16)$$

where we consider comoving radius $r = \sin\Psi$ and r_v and v are the coordinates corresponding to the generalized Vaidya spacetime. At the timelike hypersurface (Σ) where the internal and external spacetimes match with each other, Ψ becomes Ψ_b and the v and r_v become the function of comoving time t. Therefore, at Σ, we can write down the induced metric from both the sides as

$$dS_-^2|_\Sigma = -dt^2 + a^2(t)\sin^2\Psi_b d\Omega^2, \quad (17)$$

$$dS_+^2|_\Sigma = -\left(\dot{v}^2 - \frac{2M(r_v, v)}{r_v}\dot{v}^2 + 2\dot{v}\dot{r}_v\right)dt^2 + r_v^2 d\Omega^2, \quad (18)$$

where $\dot{v}$ and $\dot{r}_v$ are the partial derivatives of v and r_v with respect to comoving time t. As we know, for the smooth matching of two spacetimes at a hypersurface, the necessary and sufficient condition is that the induced metric (h_{ab}) and the extrinsic curvature (K_{ab}) from both the sides should match at the junction. From the induced metric matching of the above spacetime structures on Σ yields

$$\left(\dot{v}^2 - \frac{2M(r_v, v)}{r_v}\dot{v}^2 + 2\dot{v}\dot{r}_v\right) = 1, \quad (19)$$

$$r_v = a(t)\sin\Psi_b. \quad (20)$$

In order to calculate the extrinsic curvature (K_{ab}), one needs the information of the spacelike normal (n^α) to Σ from both the sides. From the side $\mathcal{V}^-$, the four velocity (u^α) of the comoving shell Σ can be written as $u_-^\alpha \equiv \{1, 0, 0, 0\}$. Using $(n_\alpha)_- n_-^\alpha = 1$ and $(n_\alpha)_- u_-^\alpha = 0$, we get

$$(n_\alpha)_- \equiv \{0, a(t), 0, 0\}.$$

For $\mathcal{V}^+$, we can write down the following expression of u_+^α, n_+^α as

$$u_+^\alpha \equiv \{\dot{v}, \dot{r}_v, 0, 0\}, \quad (21)$$

$$n_+^\alpha \equiv \left\{-\frac{1}{\sqrt{1 - \frac{2M}{r_v} + 2\frac{dr_v}{dv}}}, \frac{1 - \frac{2M}{r_v} + \frac{dr_v}{dv}}{\sqrt{1 - \frac{2M}{r_v} + 2\frac{dr_v}{dv}}}, 0, 0\right\}. \quad (22)$$

Using the expressions of u^α and n^α from both the sides, we get the following expressions of azimuthal components of extrinsic curvature tensors:

$$K_{\theta\theta}^- = a(t)\sin\Psi_b\cos\Psi_b, \quad (23)$$

$$K_{\theta\theta}^+ = r_v\frac{1 - \frac{2M}{r_v} + \frac{dr_v}{dv}}{\sqrt{1 - \frac{2M}{r_v} + 2\frac{dr_v}{dv}}}. \quad (24)$$

Equating $K_{\theta\theta}^+$ and $K_{\theta\theta}^-$, we get

$$\cos\Psi_b = \frac{1 - \frac{2M}{r_v} + \frac{dr_v}{dv}}{\sqrt{1 - \frac{2M}{r_v} + 2\frac{dr_v}{dv}}}. \quad (25)$$

Equating the temporal components of K_{tt} from both sides we get

$$M(r_v, v)_{,r_v} = \frac{F}{2\sin\psi_b a(t)} + \sin^2\psi_b a\ddot{a}, \quad (26)$$

where F is the Misner-Sharp mass of the internal collapsing spacetime, which should follow the following condition at the boundary:

$$F(t, \sin\psi_b) = 2M(r_v, v). \quad (27)$$

From Eq. (26), it can be seen how the flux of the matter at the boundary depends upon the scale factor and the Misner-Sharp mass (F) of the collapsing spacetime. In the present case, F is a function of time only, since it represents the internal homogeneous two-fluid system. Due to the time dependence of F, pressure is nonzero internally and it can be written as

$$p = -\frac{\dot{F}}{\dot{R}R^2}. \quad (28)$$

A nonzero pressure at the boundary of a system implies the existence of nonzero matter flux through the boundary and that is the very reason why we consider generalized Vaidya spacetime in the immediate neighborhood of the internal two-fluid system. From the above expression of pressure, it can be understood that the presence of negative pressure at the boundary of an internal spacetime implies an inward matter flux through the boundary for an expanding scenario and an outward matter flux for a collapsing scenario.

In Ref. [36], the authors defined the mass inside a spherical region, containing a fluid with energy density ρ, to be $M = \int d^3x\rho$ which in our case becomes $(4\pi/3)a^3\rho$.

It is to be noted that for the dark matter component, this mass term remains constant. For the scalar field component, this mass inside the collapsing region (within the matching surface) may vary. Figures 4 and 5 illustrate the changes in the total relativistic mass of the dark energy component produced by the phantomlike or quintessence-like scalar fields, respectively, within the boundary of the collapsing matter over comoving time. We obtain the mass of the dark energy component (quintessence and phantom field contributions) using the definition discussed in [36]. It can be seen that due to the negative equation of states of phantom and quintessence fields, mass increases during expansion (i.e., there exists an inward flow of matter) and decreases (i.e., there exists an outward flow of matter) during the collapse. In this regard we want to point out that in Ref. [37] the authors have given a detailed analysis on the effect of clustering dark energy on the halo mass at virialization. Although the models of dark energy considered in the reference have very low sound velocities and their results cannot be directly related to the present work, where the velocity of sound in the dark energy sector is unity, we opine on one or two points related to the aforementioned reference. In our model, the dark energy component has a negligible mass contribution on the dark matter halo when the system virializes, our model nearly predicts unclustered dark energy. But as in Ref. [37], the dark energy components do affect the virialization time as seen from the plots of the scale factors during the collapse. Although in our work it appears that, during the collapse, before virialization, there is some form of temporary clustering because of the nature of the variation of dark energy mass inside the spherical collapsing region, this temporary mass variation happens due to the flux of matter across the junction surface and not due to clustering nature of dark energy. Throughout the collapsing process the energy density of the dark matter component, inside the spherical patch, remains nearly constant and has nearly the same value as that of the dark energy density of the background.

In our model, the nonzero internal pressure is generated due to the presence of a scalar field, and therefore, the scalar field is responsible for the nonzero flux through the boundary. On the other hand, the matter-field part of the two-fluid system does not leak out of the boundary, since it has zero pressure. Only the scalar field continuously is leaking out/in throughout the whole dynamics of the overdense region. If there exists a nonminimal coupling between the matter and scalar field then a nonzero pressure at the boundary can make the matter-field flux out/in along with the scalar field. In this paper, we consider only the minimal coupling between the matter and scalar field, and therefore, the above-mentioned scenario where the matter has nonzero flux at the boundary is not possible. The flux of the scalar field from inside gives rise to nonzero components of the energy-momentum tensor of the external generalized Vaidya spacetime which is seeded by a fluid composed of null dust and perfect fluid. Therefore, the energy-momentum tensor of the internal spacetime and the external spacetime can be, respectively, written as

$$T^{-}_{\mu\nu} = (\rho_m + \rho_\phi + p_\phi)u^{-}_{\mu}u^{-}_{\nu} + p_\phi g^{-}_{\mu\nu},$$
$$T^{+}_{\mu\nu} = \bar{\epsilon} l_\mu k_\nu + (\epsilon + \mathcal{P})(l_\mu k_\nu + l_\nu k_\mu) + \mathcal{P} g^{+}_{\mu\nu}, \tag{29}$$

where $\bar{\epsilon}$, ϵ, and $\mathcal{P}$ can be written as

$$\bar{\epsilon} = -\frac{2M,_v}{r_v^2}, \quad \epsilon = \frac{2M,_{r_v}}{r_v^2}, \quad \text{and} \quad \mathcal{P} = -\frac{M,_{r_v r_v}}{r_v}, \tag{30}$$

and l^μ, k^μ are two null vectors which follow the condition: $l^\mu k_\mu = -1$. Due to the existence of nonzero pressure at the boundary, the flux from the internal spacetime at the boundary seeds the components of the energy-momentum tensor of the external generalized Vaidya spacetime. In the next section, we show the dynamics of the two-fluid system by solving Einstein's equations for the internal spacetime. Using the freedom to choose one free function, we consider the scalar field is either a quintessence field or a phantom field, and since the matter is minimally coupled with the scalar field, ρ_m varies as $\frac{1}{a^3}$. This prior consideration makes the matter part evolve like a closed dust ball, while the internal density of the scalar field stays almost constant throughout the evolution which implies a nonzero flux of the scalar field through the boundary. We consider the initial matter density ρ_{m_0} to be 10^3–10^4 times greater than the initial density of the scalar field which allows us to use the virialization technique discussed in Sec. II in order to understand the virialization process of the two-fluid system, though the two-fluid system in our model is not a closed system.

IV. GRAVITATIONAL COLLAPSE SOLUTIONS OF MATTER IN THE PRESENCE OF QUINTESSENCE AND PHANTOMLIKE SCALAR FIELDS

Using Einstein's equation for the FLRW spacetime [Eqs. (13) and (14)], one can write down the effective density and pressure of the resultant fluid as

$$\rho = \rho_\phi + \rho_m = \frac{1}{2}\epsilon\dot{\phi}^2 + V(\phi) + \rho_m = \frac{3\dot{a}^2}{a^2} + \frac{3k}{a^2}, \tag{31}$$

$$p = p_\phi = \frac{1}{2}\epsilon\dot{\phi}^2 - V(\phi) = -\frac{2\ddot{a}}{a} - \frac{\dot{a}^2}{a^2} - \frac{k}{a^2}, \tag{32}$$

where the $V(\phi)$ is the potential of the scalar field, ϵ is a real-valued constant, k represents the curvature of 3-space, and the overdot denotes the time derivatives of the function. In this section, the above expressions of ρ and p and all other differential equations are written in a general way, where $k = 0$ implies the corresponding equations are related to the

background, on the other hand, $k = 1$ implies they are related to the overdense region. From Eqs. (31) and (32), it can be seen that there are four unknown functions: $V(\phi), \phi(a), \dot{a}(a)$, and $\rho_m(a)$ and two differential equations, and therefore, we have the freedom to choose two free functions along with the initial conditions to solve the differential equations. As stated before, here we consider the scenario where the scalar field is minimally coupled with dustlike matter. Therefore, the energy-momentum tensors of matter and scalar field follow the conservation equation separately:

$$\nabla_a T^{ab}_{\phi} = 0 \Rightarrow \ddot{\phi} + 3\frac{\dot{a}}{a}\dot{\phi} + V_{,\phi} = 0, \tag{33}$$

$$\nabla_a T^{ab}_{m} = 0 \Rightarrow \dot{\rho}_m + 3\frac{\dot{a}}{a}\rho_m = 0. \tag{34}$$

Consequently we have $\rho_m \propto \frac{1}{a^3}$. This shows that ultimately we have to choose only one function out of $V(\phi), \phi(a), \dot{a}(a)$ to solve the differential Eqs. (31)and (32).

Using the expression of energy density and pressure of the scalar field, we can write

$$\rho_\phi + p_\phi = \epsilon\dot{\phi}^2 = \epsilon\phi^2_{,a}\dot{a}^2, \tag{35}$$

where we use the chain rule $\dot{\phi}^2 = \phi^2_{,a}\dot{a}^2$ where $\phi_{,a}$ imply a derivative with respect to a. From Eq. (31) we get

$$\dot{a} = \pm\sqrt{\frac{\rho_\phi + \rho_m}{3}a^2 - k}, \tag{36}$$

where the $+$ and $-$ signs are for expanding and collapsing scenarios, respectively. Now, differentiating (36) with respect to the comoving time (t) we get

$$\ddot{a} = \frac{a}{3}\left[\rho_\phi + \rho_m + \frac{a}{2}(\rho_{\phi,a} + \rho_{m,a})\right], \tag{37}$$

where $\rho_{\phi,a}$ and $\rho_{m,a}$ are derivatives of the scalar field energy density and the fluid energy density, respectively, with respect to the scale factor a.

Using Eqs. (35) and (36) we get

$$\rho_\phi\left(1 - \frac{\epsilon\phi^2_{,a}a^2}{3}\right) - \rho_m\frac{\epsilon\phi^2_{,a}a^2}{3} + p_\phi + k\epsilon\phi^2_{,a} = 0. \tag{38}$$

From Eq. (31) we get

$$p_\phi = \rho_\phi - 2V(\phi). \tag{39}$$

Since the quintessencelike scalar field has positive kinetic energy, $\epsilon = 1$ and we can write down the following expression of ρ_ϕ using Eqs. (38) and (39)

$$\rho_\phi = \frac{\frac{\rho_m\phi^2_{,a}a^2}{6} + V(\phi) - \frac{k\phi^2_{,a}}{2}}{\left(1 - \frac{\phi^2_{,a}a^2}{6}\right)}. \tag{40}$$

Now, using Eqs. (35)–(38), we get

$$\rho_{\phi,a} = \frac{-\phi^2_{,a}\rho_\phi a^2 - (3 + a^2\phi^2_{,a})\rho_m + 3k\phi^2_{,a}}{a} - \rho_{m,a}. \tag{41}$$

Now, differentiating Eq. (40) with respect to a and using equation Eq. (41) we get the following second order differential equation

$$\begin{aligned}
&\frac{-\phi^2_{,a}\rho_\phi a^2 - (3 + a^2\phi^2_{,a})\rho_m + 3k\phi^2_{,a}}{a} - \rho_{m,a} \\
&= \frac{1}{3(1 - \frac{\phi^2_{,a}a^2}{6})^2}\left\{3V_{,\phi}\phi_{,a} + \frac{\rho_{m,a}\phi^2_{,a}a^2}{2} + \rho_m a\phi^2_{,a}\right. \\
&\quad - \frac{\rho_{m,a}\phi^4_{,a}a^4}{12} + \rho_m\phi_{,a}\phi_{,aa}a^2 - \frac{V_{,\phi}\phi^3_{,a}a^2}{2} + V(\phi)a\phi^2_{,a} \\
&\quad \left. + V(\phi)a^2\phi_{,a}\phi_{,aa} - 3k\phi_{,a}\phi_{,aa} - \frac{k\phi^4_{,a}a}{2}\right\},
\end{aligned} \tag{42}$$

where $\phi_{,aa}$ is the second-order derivative of the scalar field with respect to a. The above second-order differential equation can also be derived from the Klein-Gordon equation of the scalar field [Eq. (33)] replacing $\ddot{\phi}$ with $\phi_{,aa}$ and $\dot{\phi}$ with $\phi_{,a}$, and using the expressions of $\dot{a}$ and ρ_ϕ written in Eqs. (36) and (40), respectively. Therefore, solving the differential Eq. (42) implies solving the Klien-Gordon equation. As we have mentioned before, we have to choose only one function among $V(\phi), \phi(a), \dot{a}(a)$ to solve the dynamics of collapse. Therefore, here, we choose $V(\phi) = V_0 e^{-\lambda\phi}$, which is generally considered as the potential of quintessencelike scalar fields [18]. This form of the potential gives accelerating expansion in FLRW models where we also have a dark matter component, as shown in Ref. [18] and consequently we have chosen this form of the scalar field potential. Any arbitrary scalar field potential (as $\frac{1}{2}m^2\phi^2$ or $\frac{1}{2}m^2\phi^2 + \frac{g}{4!}\phi^4$, for scalar field mass m and self-coupling g) does not, in general, produce accelerating expansion of FLRW models where we also have dark matter. Now, considering $V(\phi) = V_0 e^{-\lambda\phi}$, $\rho_m = \rho_{m_0}(\frac{a_0}{a})^3$, where a_0 is the initial value of scale factor and $k = 1$ we get

$$\begin{aligned}
&-4V_0 e^{-\lambda\phi}\phi_{,a}a^3 + 9\phi_{,a}a + \frac{V_0 e^{-\lambda\phi}\phi^3_{,a}a^5}{2} + \frac{\rho_{m_0}\phi^3_{,a}a^2}{4} \\
&- \phi^3_{,a}a^3 + 3\lambda a^2 V_0 e^{-\lambda\phi} - \frac{5\rho_{m_0}\phi_{,a}}{2} - \rho_{m_0}a\phi_{,aa} + 3a^2\phi_{,aa} \\
&- V_0 e^{-\lambda\phi}a^4\phi_{,aa} - \frac{\lambda V_0 e^{-\lambda\phi}\phi^2_{,a}a^4}{2} = 0,
\end{aligned} \tag{43}$$

and for $k = 0$,

$$-4V_0e^{-\lambda\phi}\phi_{,a}a^3+\frac{V_0e^{-\lambda\phi}\phi_{,a}^3a^5}{2}+\frac{\rho_{m_0}\phi_{,a}^3a^2}{4}+3\lambda a^2V_0e^{-\lambda\phi}-\frac{5\rho_{m_0}\phi_{,a}}{2}-\rho_{m_0}a\phi_{,aa}-\frac{\lambda V_0e^{-\lambda\phi}\phi_{,a}^2a^4}{2}-V_0e^{-\lambda\phi}a^4\phi_{,aa}=0, \tag{44}$$

where we consider initial scale factor value $a_0 = 1$.

We can now solve the above differential equations for $k = 0$, 1 to get the functional form of $\phi(a)$ and using the solution of $\phi(a)$ and the differential Eqs. (31) and (32), we can get the expression of scale factor a as a function of comoving time t. Since the differential Eq. (43) corresponds to $k = 1$, solving that equation and using Eqs. (31) and (32), we can get the dynamics of the resultant fluid in the overdense region. On the other hand, the solution of Eq. (44) shows the dynamics of the resultant fluid in the background, since that equation corresponds to $k = 0$.

It is generally considered that the phantomlike scalar field has negative kinetic energy and therefore, for the phantom field $\epsilon = -1$. For the phantom field, the above two differential equations become, for $k = 1$,

$$4V_0e^{-\lambda\phi}\phi_{,a}a^3-9\phi_{,a}a+\frac{V_0e^{-\lambda\phi}\phi_{,a}^3a^5}{2}+\frac{\rho_{m_0}\phi_{,a}^3a^2}{4}-\phi_{,a}^3a^3+3\lambda a^2V_0e^{-\lambda\phi}+\frac{5\rho_{m_0}\phi_{,a}}{2}+\rho_{m_0}a\phi_{,aa}-3a^2\phi_{,aa}+V_0e^{-\lambda\phi}a^4\phi_{,aa}+\frac{\lambda V_0e^{-\lambda\phi}\phi_{,a}^2a^4}{2}=0, \tag{45}$$

and for $k = 0$,

$$4V_0e^{-\lambda\phi}\phi_{,a}a^3+\frac{V_0e^{-\lambda\phi}\phi_{,a}^3a^5}{2}+\frac{\rho_{m_0}\phi_{,a}^3a^2}{4}+3\lambda a^2V_0e^{-\lambda\phi}+\frac{5\rho_{m_0}\phi_{,a}}{2}+\rho_{m_0}a\phi_{,aa}+\frac{\lambda V_0e^{-\lambda\phi}\phi_{,a}^2a^4}{2}+V_0e^{-\lambda\phi}a^4\phi_{,aa}=0, \tag{46}$$

where we consider $V(\phi) = V_0e^{-\lambda\phi}$ for the phantomlike scalar field.

The differential Eqs. (43)–(46) are second order differential equations of $\phi(a)$. Therefore, we need to consider two initial conditions $\phi(a = 1)$ and $\phi'(a = 1)$ to solve the differential equations. These initial values are chosen in such a manner that $\dot{a}$ and p_ϕ/ρ_ϕ, both of which depends on both ϕ and ϕ' attains reasonable values at the initial point when collapse starts to commence. The initial values are so chosen that p_ϕ/ρ_ϕ is near about -1 so that the scalar field sector acts like a dark energy constituent. Here we have taken the initial conditions as $\phi(a = 1) = .001$, $\phi'(a = 1) = 0.00001$ for solving the differential Eqs. (43) and (45). We have three parameters V_0, ρ_{m_0}, and λ. In our

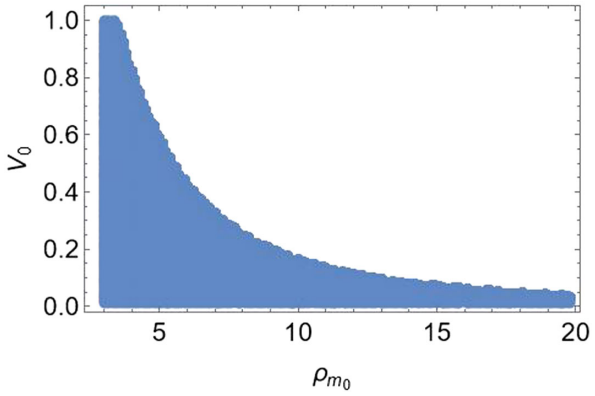

FIG. 2. Figure depicts the allowed parameters' space (i.e., shown by blue shaded region) of V_0 and ρ_{m_0} for which the overdense region collapses in the presence of quintessencelike scalar field after reaching its maximum physical radius. Both V_0 and ρ_{m_0} are expressed in inverse length squared unit. The specific nature of the unit is given in text.

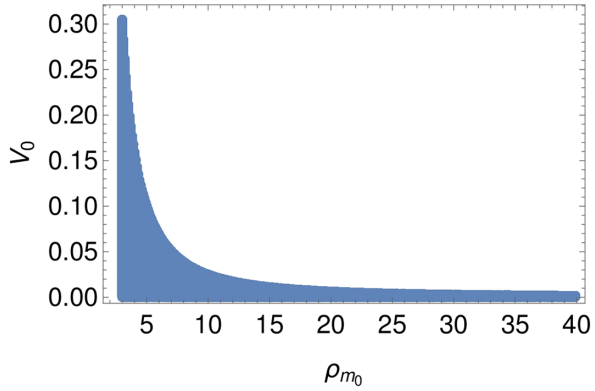

FIG. 3. Figure depicts the allowed parameters' space (i.e., shown by blue shaded region) of V_0 and ρ_{m_0} for which the overdense region collapses in the presence of phantomlike scalar field after reaching its maximum physical radius. Both V_0 and ρ_{m_0} are expressed in inverse length squared unit. The specific nature of the unit is given in text.

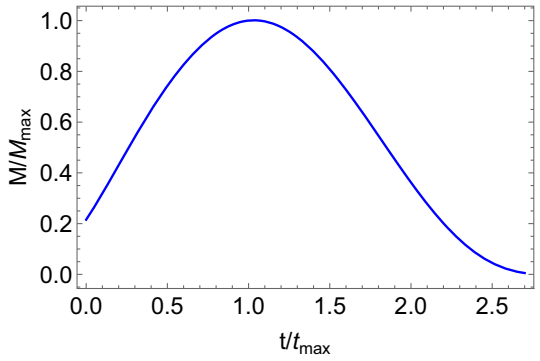

FIG. 4. Figure shows the variation of $M/M_{\max}$ with $t/t_{\max}$. Where M is the phantom contribution in mass in collapse and $M_{\max}$ is the maximum value of it and $t_{\max}$ represents the time when mass reaches its maximum value $M_{\max}$.

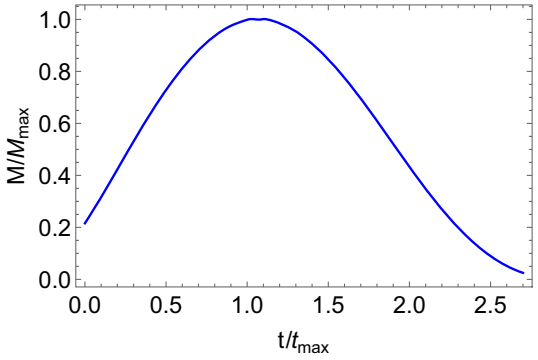

FIG. 5. Figure shows the variation of $M/M_{\max}$ with $t/t_{\max}$. Where M is the quintessence contribution in mass in collapse and $M_{\max}$ is the maximum value of it and $t_{\max}$ represents the time when mass reaches its maximum value $M_{\max}$.

geometrical system of units, the scalar field and λ are dimensionless whereas a has the dimension of length, ρ_{m_0} and V_0 have the dimensions of inverse length squared. One can choose the unit of length from the critical density of the background FLRW spacetime. In our cases we have chosen the values of ρ_{m_0} in such a way that it is always near to the critical density of the background in the epoch where collapse commences. For any particular epoch where collapse happens, if one expresses ρ_{m_0} in conventional units, then one can easily convert it into geometrized units by multiplying ρ_{m_0} by Gc^{-4} (where G is the universal gravitational constant and c is the velocity of light) and obtain a value L^{-2}, where L has the dimension of length. This value of L^{-2} can act as a suitable unit in our case to specify the values of V_0, ρ_{m_0} in Figs. 2 and 3. We have not specified the unit as we want to keep our work very general. The unit of the scale factor is not that important, as in this case only the ratio of scale factors are relevant. Given that

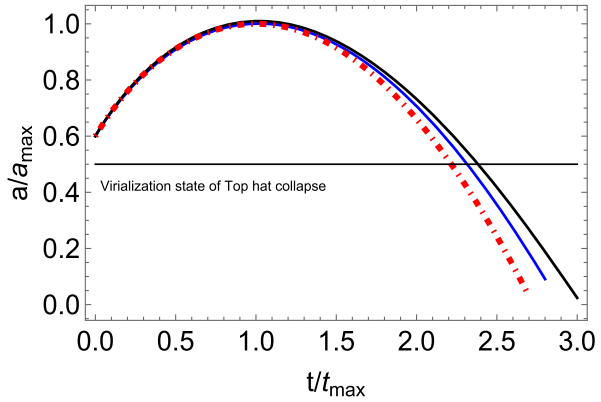

(a) Variation of a/a_{max} with t/t_{max}

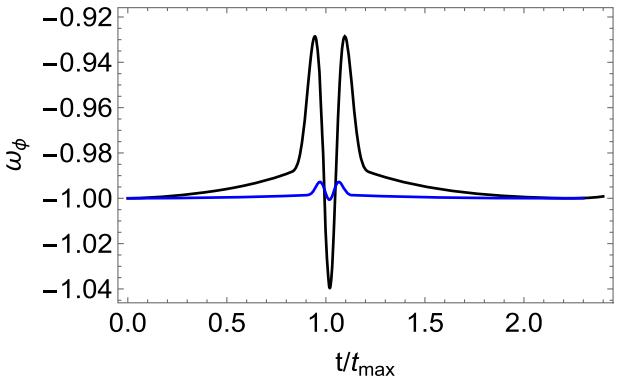

(b) Variation of ω_ϕ with t/t_{max}

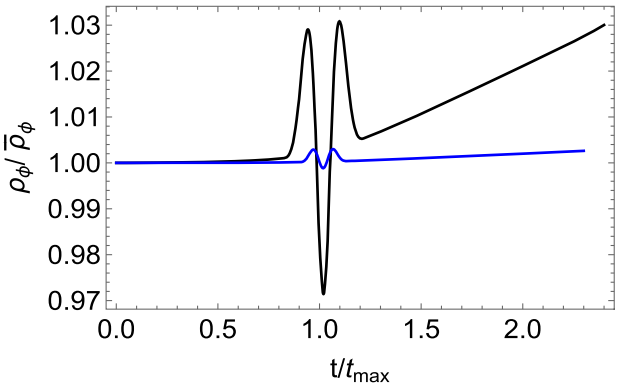

(c) Variation of $\frac{\rho_\phi}{\bar{\rho}_\phi}$ with t/t_{max}

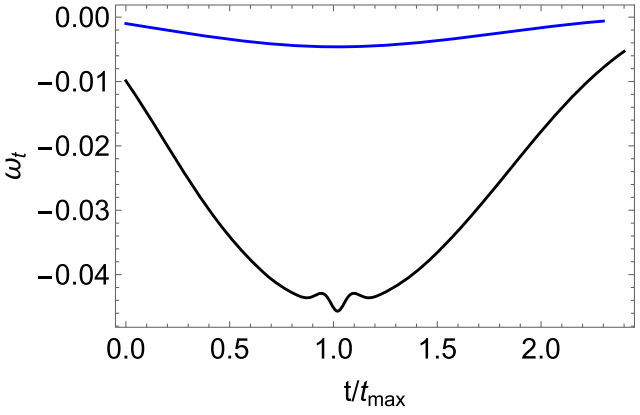

(d) Variation of ω_t with t/t_{max}

FIG. 6. Figure shows variation of different variables with variation of V_0 for scalar potential $V(\phi) = V_0 e^{-\lambda\phi}$ for quintessence field. Where $a_{\max}$ is the maximum value of scale factor and $t_{\max}$ is the time when it will reach that value. V_0 has the dimension of inverse length squared. Discussion on the unit of V_0 can be found in the main text. Here top hat collapse is represented by red dotted line whereas $\frac{V_0}{V_{\max}} = 1.01$ is represented by blue curves and $\frac{V_0}{V_{\max}} = 1.02$ is represented by the black curves. Where $V_{\max}$ is the value of $V(\phi)$ at turnaround.

the initial density of the overdense regions, ρ_{m_0}, and the background density, $\overline{\rho}_0$, have nearly identical values, any variation in the ρ_{m_0} value signifies a shift in the epoch when the primordial overdense regions begin to evolve. In order to compare our model with the standard top-hat collapse model, in this paper, we only discuss those scenarios where the initial value of $\dot{a}$ is positive. The initial positive value of $\dot{a}$ ensures an initial expansion phase of the overdense region. Now, depending on the values of the parameters V_0, ρ_{m_0}, and λ, the overdense region may reach its maximum physical radius (i.e., at the turnaround time $t = t_{\max}$) where from it starts collapsing. In Figs. 2 and 3, we show the parameters' space of V_0 and ρ_{m_0} which allows the above-mentioned dynamics of the overdense region in the presence of quintessencelike scalar field and phantomlike scalar field, respectively. In both cases, we consider $\lambda = 1$. The values of V_0 and ρ_{m_0} in the unshaded region correspond to the ever-expanding dynamics of the overdense patches.

Considering $k = 1$ and the values of V_0 and ρ_{m_0} from the shaded region of the Figs. 2 and 3, it can be shown that the solution of the end state of the gravitational collapse of the two-fluid system is a spacetime singularity. Therefore, in order to stabilize the system, like the standard top-hat collapse model, we invoke the Newtonian virialization technique in our model. In the top-hat collapse model, the matter in the overdense subuniverse is pressureless, and therefore, as discussed before, it virializes when it reaches half of its maximum physical radius. However, as discussed before, when there exist two fluids inside a compact region, and if one of them is nondust then the virialization radius may not be equal to half of the maximum physical radius. In Sec. II, we have briefly reviewed the works where the effect of dark energy on the virialization of dark matter is studied [19,21,23,25,28–34,38–43]. In the next section, we show that the scalar field behaves almost like homogeneous dark energy in our model and therefore, we can use Eq. (7) to calculate the virialization radius of the overdense region.

V. MODELING OF HOMOGENEOUS DARK ENERGY SCENARIO BY THE TWO-FLUID MODEL

As we stated before, in our model the scalar field plays the role of dark energy, and the dustlike matter is considered

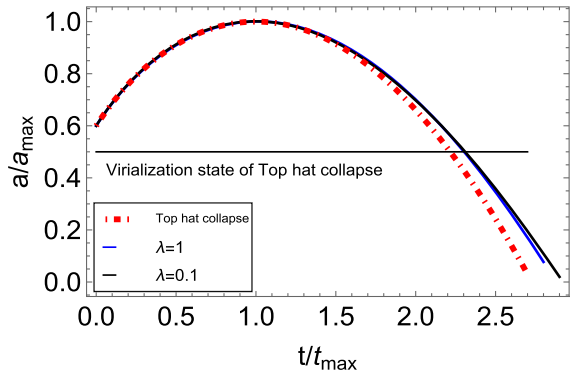

(a) Variation of a/a_{max} with t/t_{max}

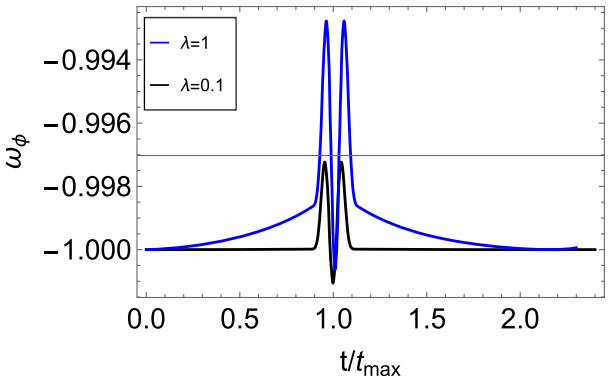

(b) Variation of ω_ϕ with t/t_{max}

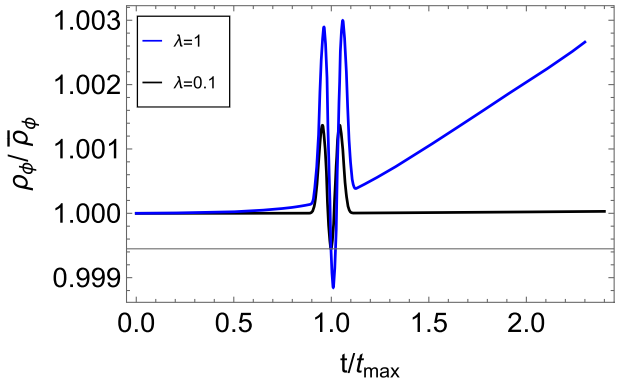

(c) Variation of $\frac{\rho_\phi}{\overline{\rho}_\phi}$ with t/t_{max}

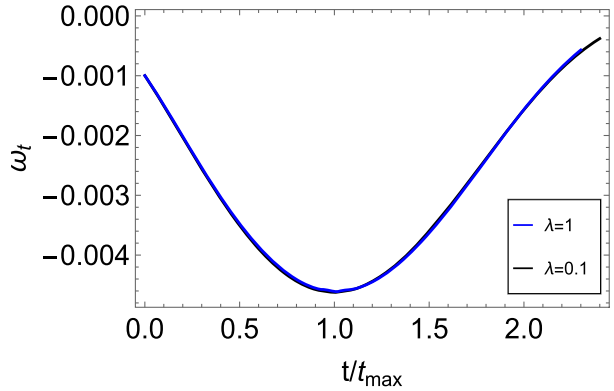

(d) Variation of ω_t with t/t_{max}

FIG. 7. Figure shows variation of different variables with variation of λ for scalar potential $V(\phi) = V_0 e^{-\lambda\phi}$ for quintessence field. Where $a_{\max}$ is the maximum value of scale factor and $t_{\max}$ is the time when it will reach that value.

dark matter. In this section, we show how the dynamics of the overdense region vary when we change the values of V_0, ρ_{m_0}, and λ. Below we list the various dynamics of the overdense region for different values of V_0, ρ_{m_0}, and λ.

In Fig. 6, we show how the dynamical quantities like $a, \omega_\phi = p_\phi/\rho_\phi, \rho_\phi/\bar{\rho}_\phi$, and $\omega_t = p_\phi/(\rho_m + \rho_\phi)$ evolve with time for different values of V_0, where ω_ϕ is the equation of state of the quintessencelike scalar field, $\rho_\phi/\bar{\rho}_\phi$ is the density ratio between the energy densities of the scalar field in the overdense region and background, and ω_t is the effective equation of state of the two-fluid system. In order to show the dynamics of the above-mentioned

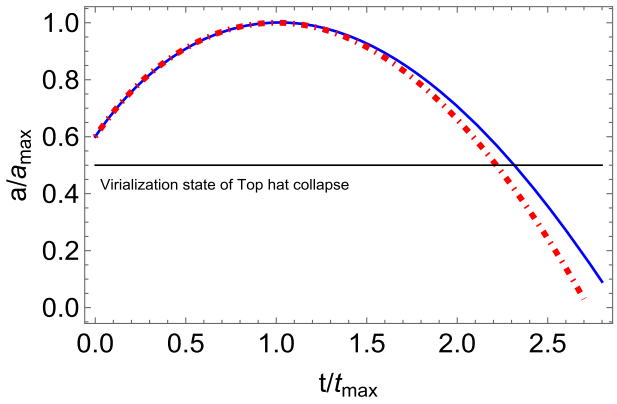

(a) Variation of a/a_{max} with t/t_{max}

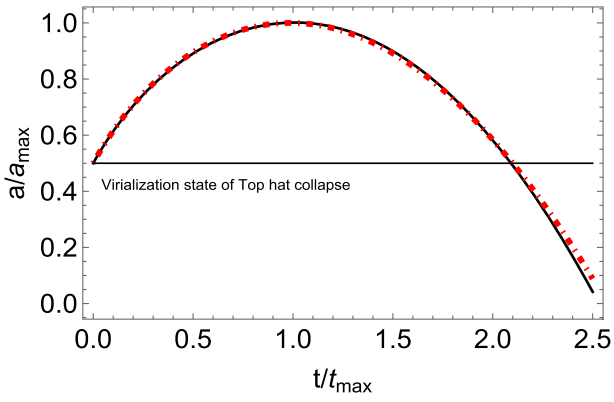

(b) Variation of a/a_{max} with t/t_{max}

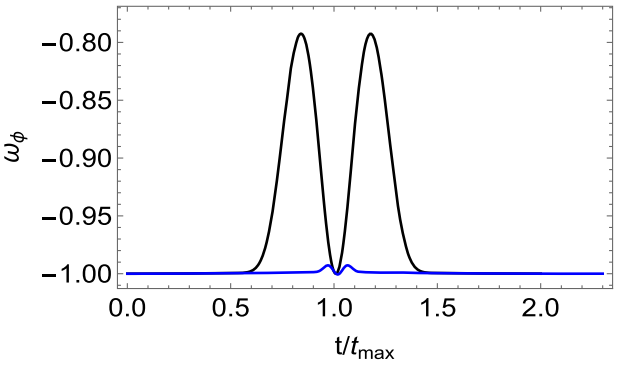

(c) Variation of ω_ϕ with t/t_{max}

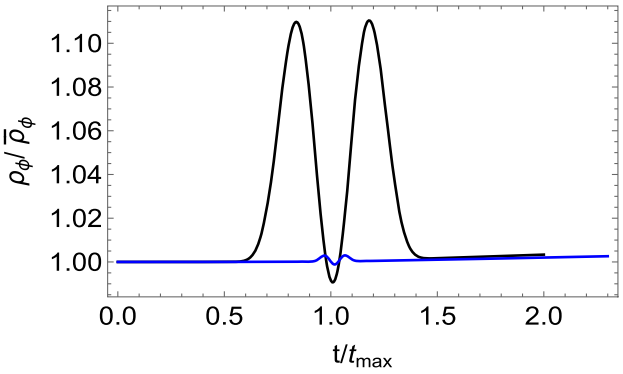

(d) Variation of $\frac{\rho_\phi}{\bar{\rho}_\phi}$ with t/t_{max}

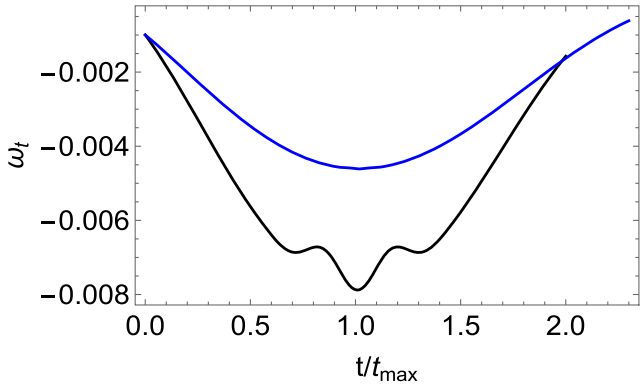

(e) Variation of ω_t with t/t_{max}

FIG. 8. Figure shows variation of different variables with variation of ρ_{m_0} for scalar potential $V(\phi) = V_0 e^{-\lambda\phi}$ for the quintessence field.Where $a_{\max}$ is the maximum value of scale factor and $t_{\max}$ is the time when it will reach that value. ρ_{m_0} has the dimension of inverse length squared. Discussion on the unit of ρ_{m_0} can be found in the main text. Here, top hat collapse is represented by red dotted line whereas $\frac{\rho m_0}{\rho_{m_{\max}}} = 24$ is represented by blue curves and $\frac{\rho m_0}{\rho_{m_{\max}}} = 50$ is represented by the black curves. Where $\rho_{m_{\max}}$ is the value of ρ_m at turnaround.

dynamical quantities for different values of V_0, we consider $\frac{\rho_{m_0}}{\rho_{m_{\max}}} = 24$, and $\lambda = 1$. From Figs. 2 and 3, it can be understood that, for a fixed value of ρ_{m0}, there exists a $\mathcal{V}_0$ such that for all values of $V_0 < \mathcal{V}_0$, the overdense region can have a collapsing phase after the initial phase of expansion. Therefore, for a fixed value of ρ_{m_0}, one cannot consider any arbitrarily large value of V_0 in order to model the desired top-hat collapselike dynamics. The above statement is also true for ρ_{m_0} since there exists a lower limit ρ_{m_0} for a fixed value of V_0. Therefore, one cannot consider arbitrary large values of both the parameters ρ_{m_0} and V_0 to model a top-hat collapselike dynamics. Hence, in our model, we consider suitable small values of these two parameters. The plots of $a, \omega_\phi, \frac{\rho_\phi}{\bar{\rho}_\phi}$, and ω_t with respect to time for $\frac{V_0}{V_{\max}} = 1.01, 1.02$ are shown in Figs. 6(a)–6(d), respectively. In Fig. 6(c), it can be seen that the density ratio $\frac{\rho_\phi}{\bar{\rho}_\phi}$ slowly increases with comoving time and stays close to one throughout the total evolution of the overdense region. The reason behind this increment of the value of the density ratio is that the background density of the scalar field decreases while the internal scalar field density approaches a constant value. However, one can consider suitable small values of V_0 to make the density ratio close to one throughout the evolution. Therefore the quintessence-like scalar field in our model approximately behaves like homogeneous dark energy. On the other hand, from Fig. 6(b), we can see that inside the overdense region, the equation of state of the scalar field $\omega_\phi \sim -1$ throughout the evolution, and that is the reason why the internal density of the scalar field approaches to a constant value. Therefore, internally, the scalar field behaves like a cosmological constant Λ. In Sec. II, we discussed the homogeneous dark energy scenario where the dark energy is the cosmological constant. For this case, the solution of η which is the ratio of virialized radius ($R_{\rm Vir}$) and the turnaround radius ($R_{\max}$) becomes

$$\eta = 0.5 - 0.25q - 0.125q^2 + \mathcal{O}(q^3),$$

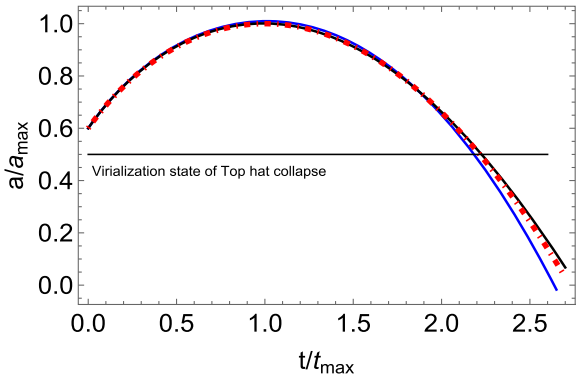

(a) Variation of a/a_{max} with t/t_{max}

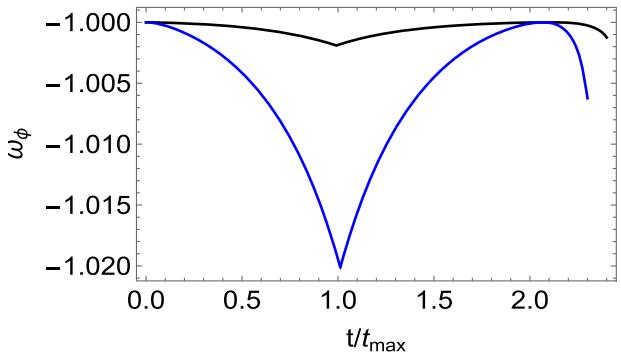

(b) Variation of ω_ϕ with t/t_{max}

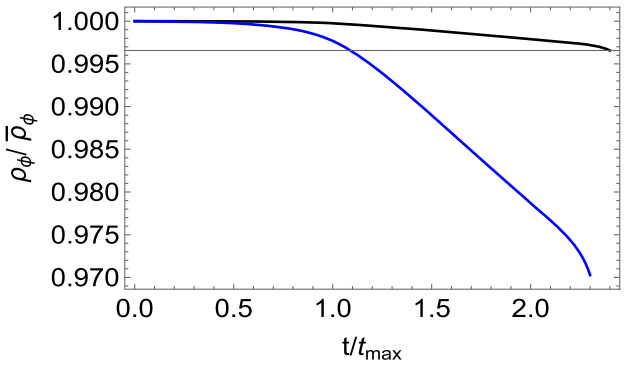

(c) Variation of $\frac{\rho_\phi}{\bar{\rho}_\phi}$ with t/t_{max}

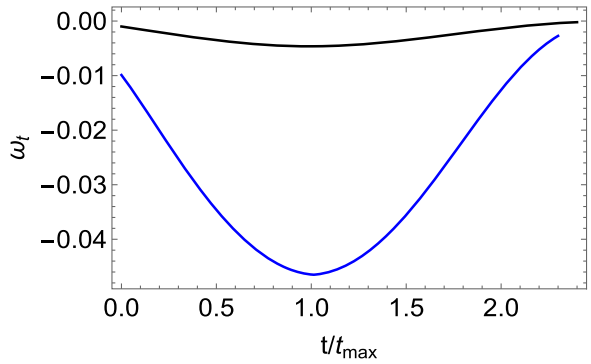

(d) Variation of ω_t with t/t_{max}

FIG. 9. Figure shows variation of different variables with variation of V_0 for scalar potential $V(\phi) = V_0 e^{-\lambda\phi}$ for the phantom field. Where $a_{\max}$ is the maximum value of scale factor and $t_{\max}$ is the time when it will reach that value. V_0 has the dimension of inverse length squared. Discussion on the unit of V_0 can be found in the main text. Here the top hat collapse is represented by red dotted line whereas for the blue curves $\frac{V_0}{V_{\max}} = 1$ with $V_0 = .01$, in inverse length squared unit, and for black curves $\frac{V_0}{V_{\max}} = 1$ with $V_0 = .001$, in inverse length squared unit. Where $V_{\max}$ is the value of $V(\phi)$ at turnaround.

where $q = (\frac{\rho_{DE}}{\rho_{DM}})_{a=a_{max}}$. In our model, at the initial stage, we get $\rho_{\phi_0} = 9.990 \times 10^{-4}$ and $\rho_{\phi_0} = 9.990 \times 10^{-3}$ for $\frac{V_0}{V_{max}} = 1.01$, 1.02, respectively. Therefore, initially, $\rho_{\phi_0}/\rho_{m_0} = 1.998 \times 10^{-4}$ for $\frac{V_0}{V_{max}} = 1.01$ and $\rho_{\phi_0}/\rho_{m_0} = 1.998 \times 10^{-3}$ for $\frac{V_0}{V_{max}} = 1.02$ which at the turnaround, becomes 4.09×10^{-3} and 4.09×10^{-2}, respectively. Therefore, in our model, the value of η does not differ much from that in the top-hat model where $\eta = 0.5$. In the top-hat model, the time interval taken by the overdense region to reach half of its maximum scale factor is 2.40. In our model, the time intervals are 2.52 and 2.79 for $\frac{V_0}{V_{max}} = 1.01$ and $\frac{V_0}{V_{max}} = 1.02$, respectively. Therefore, due to the effect of the quintessencelike scalar field, the overdense region takes larger time to virialize. Figure 6(d) shows that the total or effective equation of state (ω_t) of the two-fluid system stays close to zero throughout the evolution. It should be noted that here and throughout the remaining paper, we consider scale factor $a = 1$ at the initial time to solve the differential Eqs. (43)–(46).

In Fig. 7, we show the evolution of $a, \omega_\phi, \frac{\rho_\phi}{\bar{\rho}_\phi}$, and ω_t for $\lambda = 1$ and $\lambda = 0.1$. In this case, the values of $\frac{\rho m_0}{\rho_{m_{max}}}$ and $\frac{V_0}{V_{max}}$ are fixed at 24 and 1.01, respectively. The Figs. 7(a)–7(d) show a similar type of behavior of $a, \omega_\phi, \frac{\rho_\phi}{\bar{\rho}_\phi}$, and ω_t as we have seen in the previous case. In this case, also the ratio $\frac{\rho_\phi}{\bar{\rho}_\phi}$ stays close to one, and the $\omega_\phi \sim -1$. Consequently, for different values of λ, we can still say our model approximately resembles the homogeneous dark-energy model. Here, for $\lambda = 0.1$, at $t = 0$, we get $\rho_{\phi_0} = 9.999 \times 10^{-4}$. Therefore, at the initial stage, $\rho_{\phi_0}/\rho_{m_0} = 1.999 \times 10^{-4}$ and at turnaround time, this ratio becomes 4.2×10^{-3}. Therefore, similar to the previous case, here also the value of $\eta \sim 0.5$ and the time interval taken by the overdense region to reach the virialized radius is 2.69 that is 1.12 times greater than the virialization time in top-hat collapse model.

The same similarity can be seen in Fig. 8 where we vary the ρ_{m_0}. Therefore, observing the behavior of $a, \omega_\phi, \frac{\rho_\phi}{\bar{\rho}_\phi}$, and ω_t for all three cases, it can be concluded that our model of

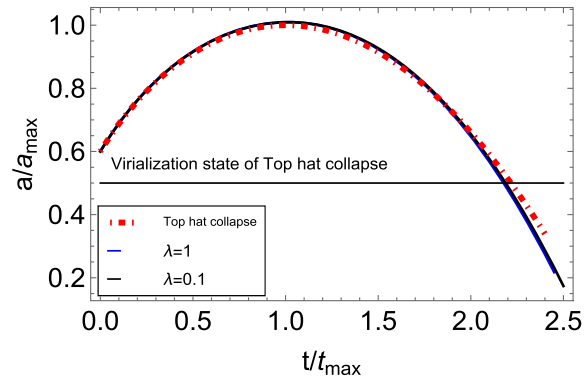

(a) Variation of a/a_{max} with t/t_{max}

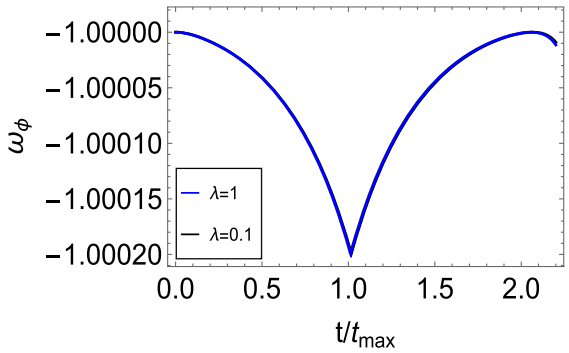

(b) Variation of ω_ϕ with t/t_{max}

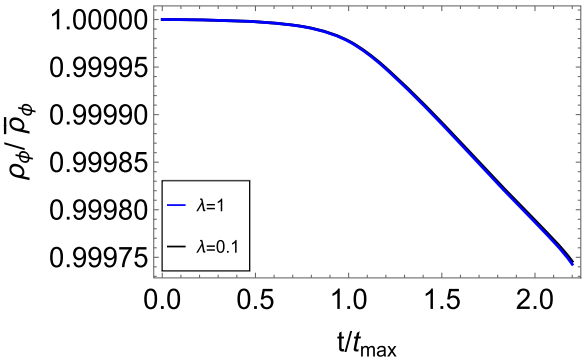

(c) Variation of $\frac{\rho_\phi}{\bar{\rho}_\phi}$ with t/t_{max}

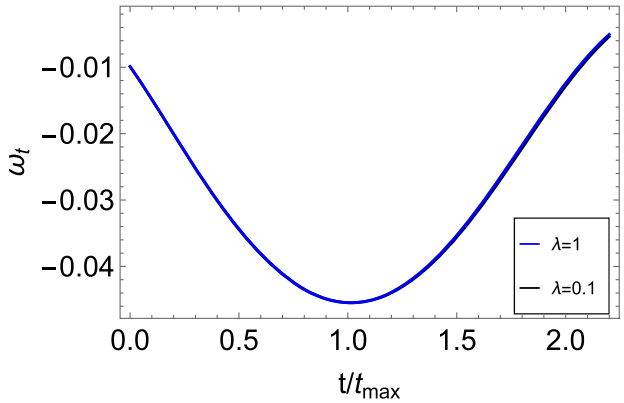

(d) Variation of ω_t with t/t_{max}

FIG. 10. Figure shows variation of different variables with variation of λ for scalar potential $V(\phi) = V_0 e^{-\lambda\phi}$ for the phantom field. Where a_{max} is the maximum value of scale factor and t_{max} is the time when it will reach that value.

two-fluid system consisting of pressureless matter and quintessencelike scalar field approximately resembles the homogeneous dark energy model.

In Figs. (9–11), we show the dynamics of $a, \omega_\phi, \frac{\rho_\phi}{\bar{\rho}_\phi}$, and ω_t for various values of V_0, λ, and ρ_{m_0} in the presence of a phantomlike scalar field. From Figs. 9(a)–9(d), 10(a)–10(d), and 11(a)–11(d), it can be seen that similar to the previous case here also $\frac{\rho_\phi}{\bar{\rho}_\phi} \sim 1$ and $\omega_\phi \sim -1$. Therefore, the phantomlike scalar field in our model also behaves like homogeneous dark energy.

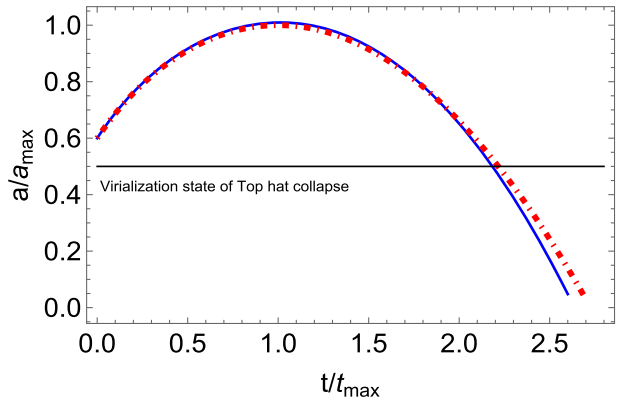

(a) Variation of a/a_{max} with t/t_{max}

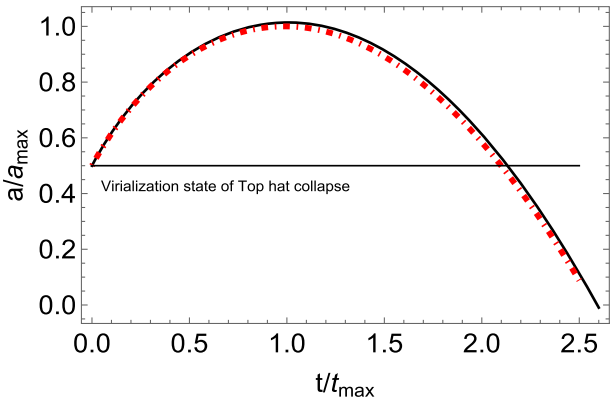

(b) Variation of a/a_{max} with t/t_{max}

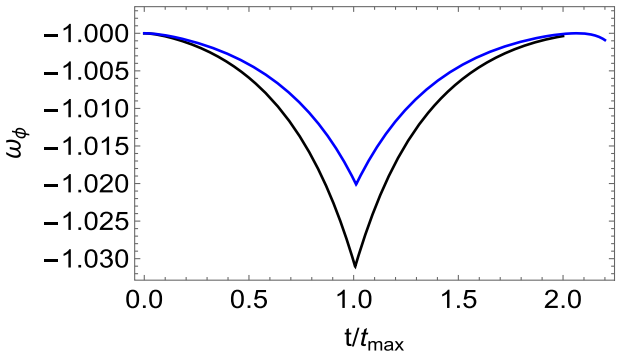

(c) Variation of ω_ϕ with t/t_{max}

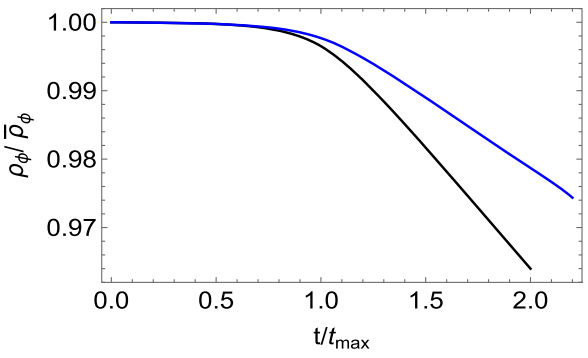

(d) Variation of $\frac{\rho_\phi}{\bar{\rho}_\phi}$ with t/t_{max}

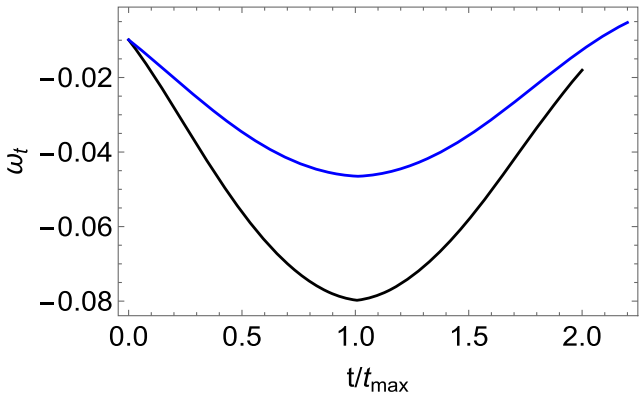

(e) Variation of ω_t with t/t_{max}

FIG. 11. Figure shows variation of different variables with variation of ρ_{m_0} for scalar potential $V(\phi) = V_0 e^{-\lambda\phi}$ for the phantom field. Where $a_{\max}$ is the maximum value of scale factor and $t_{\max}$ is the time when it will reach that value. ρ_{m_0} has the dimension of inverse length squared. Discussion on the unit of ρ_{m_0} can be found in the main text. Here, top hat collapse is represented by red dotted line whereas $\frac{\rho m_0}{\rho_{m_{\max}}} = 24$ is represented by blue curves and $\frac{\rho m_0}{\rho_{m_{\max}}} = 50$ is represented by the black curves. Where $\rho_{m_{\max}}$ is the value of ρ_m in turn around.

Till now what we have discussed deals with top-hat-like collapse in the presence of quintessence or phantomlike scalar fields. The ranges of potential parameter value and the initial matter density, which gives rise to such kind of collapse, are shown in Figs. 2 and 3. What happens if the potential parameter value and the initial matter density does not lie in the shaded region of Figs. 2 and 3? In such cases we see that our model predicts that instead of gravitational collapse, the spherical over dense patch starts to expand. These patches expand forever producing voidlike structures, inside which the matter energy density is one order less than the background matter density for some period. Later the matter density goes down. For the phantom scalar fields, it is seen that the dark energy density grows inside the spherical expanding patch, when compared with the background dark energy density. For quintessence fields the dark energy density in the spherical patch becomes less than the corresponding energy density outside of the patch. If one assumes ρ_{m_0} has a wide distribution in space for various nonlinear perturbations then, for a fixed V_0 in the shaded regions of Figs. 2, 3, one can have collapse or expansion depending on the value of ρ_{m_0}. Our work predicts that some regions of the Universe will collapse gravitationally whereas other regions will expand eternally to produce voids. For gravitational collapse of pressureless matter in the absence of scalar fields, one only obtains collapsing solutions.

VI. CONCLUSION

In this paper we have studied the gravitational dynamics of a two component system consisting of pressure-less matter and a scalar field, where the scalar field does not have any direct coupling with the matter component. The motivation to investigate this type of two-fluid dynamics is to understand how at a certain cosmological epoch, dark energy affects gravitational collapse of pressureless dark matter, where the scalar field and the pressureless matter play the role of dark energy and dark matter, respectively. We have chosen the scalar field potential in such a way that it represents the potential of quintessence- or phantomlike fields. In order to model the dynamics of the primordial overdense regions of dark matter in the presence of dark energy, we have chosen a closed FLRW metric as the internal spacetime of the overdense region which is seeded by the two component system. On the other hand, the background is modeled by flat FLRW metric which is also seeded by the two components: pressureless matter and a scalar field.

Previous authors have attempted this problem phenomenologically, where the guiding equation for the gravitational collapse of the dark matter component in presence of the scalar field was obtained from the Friedmann equations, but the complete relativistic framework was not used. The primary reason for not using the full general relativistic machinery is related to the fact that the dark energy components do not collapse with the dark matter part. In such a case one cannot use an isolated, closed FLRW spacetime which collapses towards a virial state. In the present work we have tried to implement a full general relativistic scheme to monitor the spherical collapse of the dark matter component in presence of the scalar field, up to virialization of the dark matter sector. To incorporate the relativistic treatment we have abandoned the idea of an isolated, closed FLRW spacetime collapse. Although we have used the FLRW spacetime with positive spatial curvature as the collapsing spacetime, we have matched this spacetime with an external, radiating Vaidyia spacetime at a suitable radial distance. In doing so the system has become an open system which can radiate. In order to describe a matter flux through the boundary of the overdense region, in the immediate neighborhood of the overdense region, we consider an external generalized Vaidya spacetime. We consider the potential of the scalar field $V(\phi) = V_0 e^{-\lambda\phi}$ which is the typical potential of quintessencelike and phantomlike scalar fields. We solve the Friedmann equations considering the above type of potential to investigate the dynamics of the overdense region. In order to compare our results with that of the top-hat collapse model, we restrict ourselves to investigating those scenarios where the overdense region collapses after an initial expansion phase. The collapsing spacetime is homogeneous and isotropic up to the matching radius, after which the spacetime remains isotropic but becomes inhomogeneous.

In our scheme, the collapsing dark matter affects the dark energy sector locally and induces radiation in the Vaidya region. Our work predicts that there will be overdense regions in the Universe which will not collapse, they will expand forever producing voids. Which regions will collapse and which regions will not collapse depends upon the potential parameter V_0 and the initial value of the local dark matter density ρ_{m_0}. The nature of the outgoing flux, in the Vaidya region, will depend on whether there is a collapse or an expansion. Gravitational collapse in general always produce unclustered dark energy kind of a model, where the dark energy density inside the collapsing core remains practically the same as that of the background dark energy density. On the other hand expanding patches can have clustering of dark energy as in these cases, the expanding patches have different dark energy density compared to the background spacetime. The Vaidya radiation from collapsing regions are an unique prediction of our model and in near future we will like to work on the observational side of this problem.

In this paper, we qualitatively discuss our model of spherical gravitational collapse of a two component system and do not attempt any comparison with observational data. One straightforward comparison can be done by comparing the theoretical value of the effective equation of state w_t at the virialized state with the observed equation of state of the overdense regions in the galactic cluster scale.

This comparison would give constraints on the values of V_0, λ, and ρ_{m_0} and that would be important to understand the effects of the homogeneous dark energy on structure formation at the galactic cluster scale. We will discuss this phenomenological aspect in the future.

ACKNOWLEDGMENTS

D. D. would like to acknowledge the support of the Atlantic Association for Research in the Mathematical Sciences (AARMS) for funding the work.

[1] J. H. Jeans, Phil. Trans. A. Math. Phys. Eng. Sci. **199**, 1 (1902).
[2] H. Moradpour, A. H. Ziaie, S. Ghaffari, and F. Feleppa, Mon. Not. R. Astron. Soc. **488**, L69 (2019).
[3] T. Padmanabhan, *Structure Formation in the Universe* (Cambridge University Press, Cambridge, England, 1993), ISBN: 9780521424868.
[4] J. R. Primack, arXiv:astro-ph/9707285.
[5] D. Dey and P. S. Joshi, Arab Gulf Journal of scientific research A, Mathematical and physical sciences **8**, 269 (2019).
[6] D. Dey, P. Kocherlakota, and P. S. Joshi, arXiv:1907.12792.
[7] J. E. Gunn and J. R. Gott III, Astrophys. J. **176**, 1 (1972).
[8] J. R. Oppenheimer and H. Snyder, Phys. Rev. **56**, 455 (1939).
[9] D. Garfinkle and C. Vuille, Gen. Relativ. Gravit. **23**, 471 (1991).
[10] S. S. Deshingkar, A. Chamorro, S. Jhingan, and P. S. Joshi, Phys. Rev. D **63**, 124005 (2001).
[11] M. Sharif and Z. Ahmad, Mod. Phys. Lett. A **22**, 1493 (2007).
[12] D. Markovic and S. Shapiro, Phys. Rev. D **61**, 084029 (2000).
[13] A. Del Popolo and M. Le Delliou, Galaxies **5**, 17 (2017).
[14] L. Perivolaropoulos and F. Skara, New Astron. Rev. **95**, 101659 (2022).
[15] K. Bamba, S. Capozziello, S. Nojiri, and S. D. Odintsov, Astrophys. Space Sci. **342**, 155 (2012).
[16] R. R. Caldwell, Phys. Lett. B **545**, 23 (2002).
[17] S. M. Carroll, M. Hoffman, and M. Trodden, Phys. Rev. D **68**, 023509 (2003).
[18] E. J. Copeland, M. Sami, and S. Tsujikawa, Int. J. Mod. Phys. D **15**, 1753 (2006).
[19] R. R. Caldwell, M. Kamionkowski, and N. N. Weinberg, Phys. Rev. Lett. **91**, 071301 (2003).
[20] D. Herrera, I. Waga, and S. E. Jorás, Phys. Dark Universe **26**, 100335 (2019).
[21] C. C. Chang, W. Lee, and K. W. Ng, Phys. Dark Universe **19**, 12 (2018).
[22] D. F. Mota and C. van de Bruck, Astron. Astrophys. **421**, 71 (2004).
[23] L. Wang and P. J. Steinhardt, Astrophys. J. **508**, 483 (1998).
[24] N. N. Weinberg and M. Kamionkowski, Mon. Not. R. Astron. Soc. **341**, 251 (2003).
[25] D. Dey, N. T. Layden, A. A. Coley, and P. S. Joshi, Phys. Rev. D **108**, 044046 (2023).
[26] S. Meyer, F. Pace, and M. Bartelmann, Phys. Rev. D **86**, 103002 (2012).
[27] J. Friedman and N. Stergioulas, *Rotating Relativistic Stars*, Cambridge Monographs on Mathematical Physics (Cambridge University Press, Cambridge, England, 2013).
[28] I. Maor and O. Lahav, J. Cosmol. Astropart. Phys. 07 (2005) 003.
[29] O. Lahav, P. B. Lilje, J. R. Primack, and M. J. Rees, Mon. Not. R. Astron. Soc. **251**, 128 (1991).
[30] I. T. Iliev and P. R. Shapiro, Mon. Not. R. Astron. Soc. **325**, 468 (2001).
[31] C. Horellou and J. Berge, Mon. Not. R. Astron. Soc. **360**, 1393 (2005).
[32] S. Basilakos, Astrophys. J. **590**, 636 (2003).
[33] S. Basilakos and N. Voglis, Mon. Not. R. Astron. Soc. **374**, 269 (2007).
[34] S. Basilakos, J. Bueno Sanchez, and L. Perivolaropoulos, Phys. Rev. D **80**, 043530 (2009).
[35] The generalized Vaidya spacetime is a natural contender for the external spacetime because it is the simplest, spherically symmetric, solution of the Einstein equation which admits of null radiation and matter flux. As we expect the external spacetime to absorb the energy flux from the internal FLRW region, we choose the generalized Vaidya spacetime as the external spacetime.
[36] P. Creminelli, G. D'Amico, J. Norena, L. Senatore, and F. Vernizzi, J. Cosmol. Astropart. Phys. 03 (2010) 027.
[37] R. C. Batista and V. Marra, J. Cosmol. Astropart. Phys. 11 (2017) 048.
[38] W. J. Percival, Astron. Astrophys. **443**, 819 (2005).
[39] N. J. Nunes and D. F. Mota, Mon. Not. R. Astron. Soc. **368**, 751 (2006).
[40] P. Wang, Astrophys. J. **640**, 18 (2006).
[41] I. Maor, Int. J. Theor. Phys. **46**, 2274 (2007).
[42] S. Basilakos, M. Plionis, and J. Sola, Phys. Rev. D **82**, 083512 (2010).
[43] S. Lee and Kin-Wang Ng, J. Cosmol. Astropart. Phys. 10 (2010) 028.